2

One-dimensional diffusion based solidification model with volumetric expansion and shrinkage effect: semi-analytical approach

2.1 INTRODUCTION

Volumetric expansion and shrinkage due to different densities of solid and liquid phases are common phenomena during solidification process. Simple analytical models addressing effect of volumetric expansion/shrinkage during solidification are rarely found. The few existing 1-D solidification models are valid only for semi-infinite domain with limitations of their application for finite domain size. The focus of the present chapter is to develop a 1-D semi-analytical solidification model addressing effects of volumetric expansion/ shrinkage in a finite domain. The proposed semi-analytical scheme involves finding simultaneous solution of transient 1-D heat diffusion equations at solid and liquid domain coupled at the interface by Stefan condition.

Mathematical prediction of macroscopic phase change processes have emerged to be of utmost importance for various engineering applications such as manufacturing processes involving casting and welding, latent heat based thermal storage, and thermal management of electronic devices, pharmaceuticals, buildings and many more. In general, phase change processes are transient in nature and involves moving interface. The growth rate of interface depends on heat transfer rate, convection, and shrinkage or volumetric expansion due to different densities of solid and liquid phases. 2-D and 3-D numerical models involving influence of convection and shrinkage on solidification process have been widely studied and reported by several authors Wang et al. [2005]; Ni and Beckermann [1991]; Voller et al. [1987]; Chiang and Tsai [1992b,a]; Kim and Ro [1993]; Xu and Li [1991]; Magnusson and Arnberg [2001]; Pequet et al. [2002]; Sun and Garimella [2007]. However, very few of the reported models involves simple diffusion based analytical approach and those few models are valid only for semi-infinite domain [Worster, 1986; Rappaz and Dantzig, 2009; Natale et al., 2010]. Worster [1986] developed a 1-D analytical model for solidification of alloys for semi-infinite domain and captured the growth of mushy layer for aqueous salt solution. Rappaz and Dantzig [2009] reported an analytical model for solidification of pure substance in a mould, however the model involves semi-infinite consideration for the liquid domain. Recently, Chakraborty and Dutta [2003] employed an analytical model involving quasi-steady state and semi-infinite consideration and studied cyclic melting and freezing of phase change materials (PCM) used for thermal management of electronic device. More recently, Natale et al. [2010] proposed explicit analytical solutions for one-dimensional two-phase free boundary problems considering shrinkage and volumetric expansion. Once again, solution involves semi infinite formulation for liquid phase, and the report although discussed the theory, it is devoid of any case study.

Among the reports concerning 2-D and 3-D numerical modeling, Bennon and Incropera [1987a,b] proposed a numerical scheme based on volume averaged continuum model for solidification of binary alloys. Voller et al. [1987] and Brent et al. [1988] proposed fixed grid based enthalpy updating scheme to capture growing solid-liquid interface during solidification. Recently, Chakraborty [2017] proposed a modification of enthalpy updating scheme originally proposed by Voller et al. [1987] and Brent et al. [1988] to address solidification with large difference

in specific heats for solid and liquid phases.

Since analytical model involving shrinkage or volumetric expansion has rarely received research attention [Natale et al., 2010], the present study is aspired toward developing an semi-analytical model of solidification considering effect of difference in solid-liquid phase densities, and valid for finite domain. The moving interface due to solid-liquid phase transition is addressed by conservation of mass and energy at the interface, while the change in total domain length due to volumetric expansion or shrinkage is tackled by considering overall mass balance for the combined solid and liquid domain. In order to validate the proposed model for finite domain, solidification of water without considering volumetric expansion (same density for solid and liquid phase) has been studied, and results are compared with those obtained from existing enthalpy updating based numerical model [Voller et al., 1987; Brent et al., 1988; Chakraborty, 2017]. Once the validation provided reasonable agreement indicating the robustness of the proposed model, case studies corresponding to volumetric expansion and shrinkage (different densities for solid and liquid phases) are described. Results are discussed for two different case studies namely (i) solidification of water involving volumetric expansion and (ii) solidification of paraffin (P116) involving shrinkage.

2.2 MATHEMATICAL MODEL

The generic problem to be studied for the present chapter is shown in figure 2.1, where liquid PCM initially at a temperature (T_i) greater than its melting temperature T_m is placed inside an insulated cavity. As the bottom surface is exposed to a cold temperature (T_c<T_m) and maintained at T_c, solidification ensues from the bottom surface. For the entire process all the remaining surfaces barring the bottom surface are kept insulated. The bottom cooling orientation is particularly chosen as it ensures complete suppression of free convection in the liquid domain for most of the pure substances or eutectic solutions. Even with bottom cooled orientation, free convection might ensue due to density anomaly of water around 4 ^oC, or due to shrinkage induced flow [Chiang and Tsai, 1992b,a]. However, effect of such convection can be considered sufficiently negligible if the hydraulic diameter of the cavity based on the area perpendicular to the direction of solidification is much smaller than the length scale along the direction of solidification. In the absence of free convection or shrinkage induced flow, the heat transfer process can be completely attributed to the diffusion mechanism.

The heat transfer model involving phase change process belongs to a special class of heat transfer problems predominantly recognized as “Stefan problem” or moving interface problem. Two boundaries of the solid domain are defined by the fixed cold surface at the bottom (figure 2.1) and the moving solid–liquid interface at top. On the other hand the boundaries of the liquid domain are defined by the moving solid-liquid interface at bottom and the moving end at the top due to volumetric expansion or shrinkage. Hence, both the boundaries associated with the liquid domain are moving boundaries. Even though, these problems have extensive applications, the analytical solutions are available only for semi-infinite domain. In the present model, the solidification domain is diligently chosen to be finite, and a rigorous step-by-step semi-analytical approach is developed to address solidification process involving shrinkage or volumetric expansion.

The model is developed with the following assumptions: (i) phase change process is driven by 1-D heat diffusion mechanism, (ii) material properties of solid and liquid phases are different, although individual phase properties does not vary with temperature and considered to be constants, and (iii) hydraulic diameter corresponding to the cavity cross section is small enough with respect to the cavity height so that convection due to density anomaly of water and shrinkage induce flow is negligible. With these assumptions the 1-D heat diffusion equation for each of the

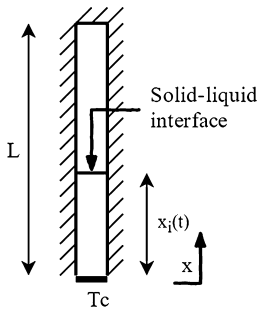

Figure 2.1 : Mathematical model of generic problem.

phases can be written as:

$$\frac{\partial T_\phi}{\partial t} = \alpha_\phi \frac{\partial^2 T_\phi}{\partial x^2} \tag{2.1}$$

where, $\alpha_\phi = k_\phi / \rho_\phi c_{p_\phi}$ is thermal diffusivity of PCM, and subscript $\phi = l, s$ represents liquid and solid phases respectively. For the solid domain the boundary conditions are: $T(0,t) = T_c$ and $T(x_i,t) = T_m$ while, for liquid domain the boundary conditions are: $T(x_i,t) = T_m$ and $\partial T/\partial x|_{x=L} = 0$. $T_{\phi=l,s}$ appearing in Eq. 2.1 represents temperature distribution at solid and liquid domains, and x_i represents the solid liquid interface. In order to address the effect of different densities of solid and liquid ($\rho_s \neq \rho_l$), mass conservation must be used to identify the interface location $x_i(t)$ as well as the total length of the domain $L(t)$. Since the mass of solid after solidification must be equal to mass of liquid before solidification ($dm_s = dm_l$), for constant cross-sectional area(A): $\rho_s dx_s = \rho_l dx_l$, where differential volume of solid and liquid phases are given by $dv_\phi = A dx_\phi$. $T_{\phi=s,l}$ in solid and liquid domain are coupled through Stefan condition or the energy balance at the interface. Noting the fact $\rho_s dx_s = \rho_l dx_l$, the energy balance equation at the interface can be written as:

$$\rho_s h_{sl} \frac{dx_i}{dt} = k_s \left.\frac{\partial T_s}{\partial x}\right|_{x_i} - k_l \left.\frac{\partial T_l}{\partial x}\right|_{x_i} \tag{2.2}$$

where, h_{sl} denotes latent heat of solidification. In a similar fashion, mass balance for the entire domain at consecutive time interval provides the formulation for finding the total length $L^{(k)}$ at a given time instant as follows:

$$L^{(k)} = L^{(k-1)} + \left(1 - \frac{\rho_s}{\rho_l}\right)\left(x_i^{(k)} - x_i^{(k-1)}\right) \tag{2.3}$$

where, superscript (k) and $(k-1)$ represent present and previous time-steps.

Although, the boundary conditions for this problem are well defined, implementing initial condition, particularly for the solid domain poses a severe limitation. As the cavity is initially filled with liquid phase, initial condition for the liquid domain is straight forward and can be considered as $T(x,0) = T_i > T_m$. However, obtaining the initial condition for solid domain is not so trivial as solid phase does not even exist at time $t = 0$. To circumvent the ill posed nature of initial condition for the solid domain, the semi-infinite solution can still be used for an extremely small initial time-step during which semi-infinite consideration is valid. The semi-infinite formulation considers the boundary conditions as being $T|_{x=0} = T_c$ and $T|_{x\to\infty} = T_i$, and temperature at the liquid domain asymptotically reaches T_i. When the semi-infinite formulation (Eq. 2.4-2.6) reported by Rappaz and Dantzig [2009] is used for a very small time-step of $\Delta t = 10^{-6}$ s, the length scale over which this asymptotic temperature profile is achieved is found out to be of the order of $O{\sim}10^{-3} - 10^{-4}$ mm, which is much smaller than the overall length-scale of the solidification domain under consideration ($O{\sim}10$ mm). Hence, validity of semi-infinite formulation during the initiation of solidification for such small time-step can be considered to be reasonable. A time-step of

$\Delta t = 10^{-6}\ s$ is considered to allow the growth of the initial solid domain, and temperature profile of the solid and liquid domains are obtained by the following semi-infinite formulations [Rappaz and Dantzig, 2009].

$$T_s(x,t) = T_c + \frac{(T_m - T_c)}{erf(\zeta)} erf\left(\frac{x}{2\sqrt{\alpha_s t}}\right) \quad 0 \leqslant x \leqslant x_i \tag{2.4}$$

$$T_l(x,t) = T_i - \frac{(T_i - T_m)}{erfc\left(\zeta\sqrt{\frac{\alpha_s}{\alpha_l}}\right)} erfc\left(\frac{x}{2\sqrt{\alpha_l t}}\right) \quad x_i \leqslant x \leqslant \infty \tag{2.5}$$

$$x_i = 2\zeta\sqrt{\alpha_s t} \tag{2.6}$$

ζ is unknown and is obtained numerically after substituting Eq. 2.4, Eq. 2.5 and Eq. 2.6 in Stefan equation (Eq. 2.2). Once the $T_{\phi=s,l}$ are obtained along with x_i at time $t = 10^{-6}\ s$ from Eq. 2.4-2.6, this information can be used as initial condition for subsequent time steps.

In order to obtain close form solution in terms of non-dimensional (ND) temperature profile, Eq. 2.1 is non-dimensionlized considering dimensionless: temperature $\theta_\phi = (T_\phi - T_c)/(T_i - T_c)$, distance $X = x/L_0$ and time $F_o = \alpha_l t/L_0^2$ where, L_0 and α_l are initial length of the liquid phase ($L_0 = L|_{t=0}$) and thermal diffusivity corresponding to liquid region.

$$\frac{\partial\theta_\phi}{\partial F_o} = \alpha_\phi^* \frac{\partial^2\theta_\phi}{\partial X^2} \tag{2.7}$$

α_ϕ^* appearing in 2.7 is defined as $\alpha_\phi^* = \alpha_\phi/\alpha_l$. Representing ND interface location as $X_i^*(F_o) = x_i(F_o)/L_0$ and non dimensional overall length as $L^*(F_o) = L(F_o)/L_0$, the modified ND initial and boundary conditions pertaining solid domain for the subsequent time-steps can be written as: $\theta_s(X,0) = \theta_s(X,10^{-6})$ obtained from Eq. 2.4, and $\theta_s(0,F_o) = 0$, $\theta_s(X_i^*,F_o) = \theta_m$ respectively. Similarly for the liquid domain initial condition for subsequent time-step is $\theta_l(X,0) = \theta_l(X,10^{-6})$ obtained from Eq. 2.5, $\theta_l(X_i^*,F_o) = \theta_m$ and $\partial\theta_l/\partial X|_{X=L^*} = 0$, where, $\theta_m = (T_m - T_c)/(T_i - T_c)$. The initial interface location $X_i^*|_{t=0} = x_i|_{t=10^{-6}}/L_0$ can be obtained from Eq. 2.6. The ND form of Stefan equation (Eq. 2.2) can be expressed as follows.

$$\frac{dX_i^*}{dF_o} = \beta_s\alpha_s^* \left.\frac{\partial\theta_s}{\partial X}\right|_{X_i^*} - \beta_l\alpha_l^* \left.\frac{\partial\theta_l}{\partial X}\right|_{X_i^*} \tag{2.8}$$

where, $\beta_\phi = \rho_\phi c_{p\phi}(T_i - T_c)/\rho_s h_{sl}$. Similarly the overall length updating formulation reduces to the following non dimensional form.

$$L^{*(k)} = L^{*(k-1)} + \left(1 - \frac{\rho_s}{\rho_l}\right)\left(X_i^{*(k)} - X_i^{*(k-1)}\right) \tag{2.9}$$

It is pertinent to mention here that $L^*|_{t=0} = 1$ and for shrinkage ($\rho_s > \rho_l$): L^* will evolve into a value < 1 as solidification ensues, and reverse is true for volumetric expansion ($\rho_s < \rho_l$) (*i.e* $L^* > 1$ as solidification proceeds). Also, change in L^* can be considered to be negligible during evaluation of initial T_ϕ distribution and x_i by using semi-infinite formulation (Eq. 2.4-2.6) for an extremely small time step ($\Delta t = 10^{-6}\ s$).

A recent study by Chakraborty et al. [2017] on semi-analytical modeling of droplet evaporation revealed that a time-step based treatment of initial condition is capable of producing better accuracy in solutions if the problem deals with phase transition involving moving interface or moving boundary conditions. Following the same line of action, the initial condition for a particular time-step is adopted from the solution obtained at previous time-step. The system of equations described by Eq. 2.7-2.9 needs to be solved simultaneously to obtain θ_ϕ profile and X_i^*.

If we denote the present time step with superscript (k) and previous time step with superscript $(k-1)$ then the analytical solution of heat diffusion Eq. 2.7 for solid and liquid domains for the present time-step ($\Delta F_o^{(k)}$) can be written as:

$$\theta_s^{(k)} = \frac{\theta_m X}{X_i^{*(k)}} + \sum_{n=1}^{\infty} \exp\left(\frac{-\alpha_s^* n^2 \pi^2 \Delta F_o^{(k)}}{X_i^{*(k)2}}\right) \sin\left(\frac{n\pi X}{X_i^{*(k)}}\right) C_n \qquad 0 \leqslant X \leqslant X_i^{*(k)} \tag{2.10}$$

$$\theta_l^{(k)} = \theta_m + \sum_{n=1}^{\infty} \exp\left(\frac{-(2n-1)^2 \pi^2 \Delta F_o^{(k)}}{4(L^{*(k)} - X_i^{*(k)})^2}\right) \sin\left(\frac{(2n-1)\pi(X - X_i^{*(k)})}{2(L^{*(k)} - X_i^{*(k)})}\right) D_n$$
$$X_i^{*(k)} \leqslant X \leqslant L^{*(k)} \tag{2.11}$$

Where, $\theta_{\phi=s,l}^{(k)}$ represents non dimensional temperature distribution in the solid and liquid domain at (k)th time step. C_n and D_n appearing in Eq. 2.10 and Eq. 2.11 depends on ND temperature distribution obtained by solving at previous time step $\Delta F_o^{(k-1)}$ and are defined as follows:

$$C_n = \frac{2}{X_i^{*(k-1)}} \int_0^{X_i^{*(k-1)}} \left(\theta_s^{(k-1)} - \frac{\theta_m X}{X_i^{*(k-1)}}\right) \sin\left(\frac{n\pi X}{X_i^{*(k-1)}}\right) dx \tag{2.12}$$

$$D_n = \frac{2}{(L^{*(k-1)} - X_i^{*(k-1)})} \int_{X_i^{*(k-1)}}^{L^{*(k-1)}} \left(\theta_l^{(k-1)} - \theta_m\right) \sin\left(\frac{(2n-1)\pi(X - X_i^{*(k-1)})}{2(L^{*(k-1)} - X_i^{*(k-1)})}\right) dx \tag{2.13}$$

Where, $\theta_\phi^{(k-1)}$, $X_i^{*(k-1)}$ and $L^{*(k-1)}$ are obtained at previous time step $\Delta F_o^{(k-1)}$. Formulation for $X_i^{*(k)}$ at current time-step can be obtained by substitution of $\theta_\phi^{(k)}$ (Eq. 2.10, 2.11) in Eq. 2.8.

$$\frac{dX_i^*}{dF_o} = \frac{\beta_s \alpha_s^* \theta_m}{X_i^{*(k)}} + \frac{\beta_s \alpha_s^*}{X_i^{*(k)}} \sum_{n=1}^{\infty} (-1)^n n\pi \exp\left(\frac{-\alpha_s^* n^2 \pi^2 \Delta F_o}{X_i^{*(k)2}}\right) C_n$$
$$- \frac{\beta_l \alpha_l^*}{(L^{*(k)} - X_i^{*(k)})} \sum_{n=1}^{\infty} \frac{(2n-1)\pi}{2} \exp\left(\frac{-(2n-1)^2 \pi^2 \Delta F_o}{4(L^{*(k)} - X_i^{*(k)})^2}\right) D_n \tag{2.14}$$

Once the required formulations for θ_ϕ, X_i^* and L^* are obtained from system of Eq. 2.9-2.14, the semi-analytical approach can be described by the following steps:

1. Obtain the initial θ_ϕ and X_i^* from semi-infinite solutions given by Eq. 2.4-2.6 for a very small time step ($\Delta t = 10^{-6}\ s$ is used for the present study). Since the effect of shrinkage or volumetric expansion are negligible for such small time scale, change of L^* can be considered to be negligible for this initial evaluation.

2. Using these initial θ_ϕ and X_i^* obtain C_n and D_n using numerical integration of Eq. 2.12 and 2.13.

3. Obtain X_i^* and L^* by simultaneously solving Eq. 2.14 and Eq. 2.9 in an iterative manner. Eq. 2.14 can be solved using iterative Euler's method described as follows:

$$X_{i(j)}^{*(k)} = X_i^{*(k-1)} + 0.5[f^{(k-1)} + f_{(j-1)}^{(k)}]\Delta F_o^{(k)} \tag{2.15}$$

Where, subscript (j) is iteration step, superscript (k) represents time-step. $f_{(j-1)}^{(k)} = f^{(k)}(X_{i(j-1)}^*, L_{(j-1)}^*)$ represents right hand side of Eq. 2.14, and $f^{(k-1)}$ represents the same at previous time-step. The first guess for $f_{(0)}^{(k)}$ can be considered to be $f^{(k-1)}$ value from the previous time-step. Updating of $L_j^{*(k)}$ can be obtained by using Eq. 2.9. Repeat step 3 till convergence for $X_i^{*(k)}$ and $L^{*(k)}$ is obtained ($X_{i(j)}^{*(k)} - X_{i(j-1)}^{*(k)} \leq 10^{-6}$ and $L_{(j)}^{*(k)} - L_{(j-1)}^{*(k)} \leq 10^{-6}$).

4. Update $\theta_\phi^{(k)}$ using Eq. 2.10- 2.11.

5. For subsequent time-steps C_n and D_n can be calculated by direct substitution of Eq. 2.10 and 2.11 in Eq. 2.12 and 2.13 respectively which provides following simplified recursive expressions for C_n and D_n.

$$C_n^{(k)} = \exp\left(\frac{-\alpha_s^* n^2 \pi^2 \Delta F_o}{X_i^{*(k-1)^2}}\right) C_n^{(k-1)} \tag{2.16}$$

$$D_n^{(k)} = \exp\left(\frac{-(2n-1)^2 \pi^2 \Delta F_o}{4\left(L^{*(k-1)} - X_i^{*(k-1)}\right)^2}\right) D_n^{(k-1)} \tag{2.17}$$

6. For subsequent time-intervals follow the described steps in the order 5, 3, and 4 to update $X_i^{*(k)}$, $L^{*(k)}$, and $\theta_\phi^{(k)}$.

Steps 1-6 concludes the semi-analytical scheme to obtain θ_ϕ, X_i^* and L^* during 1-D directional solidification in finite domain.

2.3 VALIDATION AND CASE STUDIES

To validate this newly developed scheme, solidification of water without considering volumetric expansion (*ie.* $\rho_l = \rho_s = 1000\, kg/m^3$) is considered. The other thermo-physical properties of water are considered to be: $k_l = 0.6\ W/mK$, $k_s = 2.3\ W/mK$, $c_{ps} = 2000\ J/kgK$, $c_{pl} = 4000\ J/kgK$, $h_{sl} = 335\ kJ/kg$, and $T_m = 273.16\ K$, while initial temperature, cold side temperature and length of the domain are chosen to be $T_i = 283.16\ K$, $T_c = 263.16\ K$ and $L = 20\ mm$. It is pertinent to mention here that the overall length of the domain is no longer time independent (*ie.* $L \neq f(t)$) if $\rho_l = \rho_s$, so that Eq. 2.3 and 2.9 become redundant and L^* appearing in Eq. 2.10-2.17 can simply be replaced by $L^* = 1$. The results obtained from proposed semi-analytical are compared with the numerical results obtained from enthalpy updating scheme proposed by Voller et al. [1987]; Brent et al. [1988], and Chakraborty [2017]. The reference numerical model involves solving a single volume averaged energy equation (Eq. 2.18) [Chakraborty, 2017] which is valid for the entire domain consisting of fully solid phase, fully liquid phase as well as interface where liquid and solid phases coexist.

$$\frac{\partial T}{\partial t} = \frac{\partial}{\partial x}\left(\frac{k}{\rho c_{ps}}\left(\frac{\partial T}{\partial x}\right)\right) - \frac{h_{sl}}{c_{ps}}\frac{\partial f_l}{\partial t} - \left(\frac{c_{pl}}{c_{ps}} - 1\right)\frac{\partial}{\partial t}\left[f_l(T - T_m)\right] \tag{2.18}$$

In Eq. 2.18, $k = f_l k_l + (1 - f_l)k_s$ represents volume averaged thermal conductivity, and $0 \leq f_l \leq 1$ represents liquid volume fraction. Solution of Eq. 2.18 involves simultaneous evaluation of T and f_l using enthalpy updating scheme proposed by Chakraborty [2017].

Variation of X_i^* with F_o and spatial distribution of θ_ϕ at $t = 150s$ obtained from the proposed semi-analytical model and reference numerical model [Chakraborty, 2017] are compared and shown in figure 2.2(a) and (b). The absolute difference between predicted θ_ϕ by these two models are also plotted along the direction of solidification for different time instants and shown in figure 2.3. The inset in figure 2.3 also shows the absolute difference between dimensional temperature (T_ϕ) predicted by these two models. From these comparisons it is evident that difference between X_i^* obtained by these two models is of the order of $\sim 100\ \mu m$. On the other hand θ_ϕ agrees within 6.5% of accuracy for these two models, and maximum difference in T_ϕ is found out to be close to $\sim 1\ ^oC$. The difference between the predicted results by these two models can be attributed to their inherent solution approach. While the proposed model addresses the coupling of temperature distributions in solid and liquid domain through interface by means of Stefan

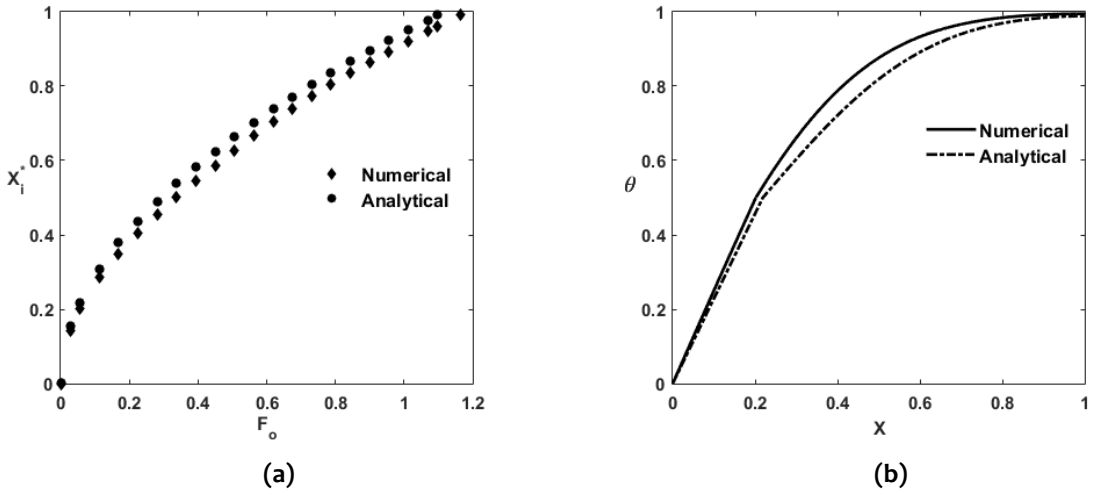

Figure 2.2 : (a) Comparison of predicted solid–liquid interface (X_i^*) evolution in time by proposed model with numerical model, and (b) spatial variation of ND temperature at $t = 150s$.

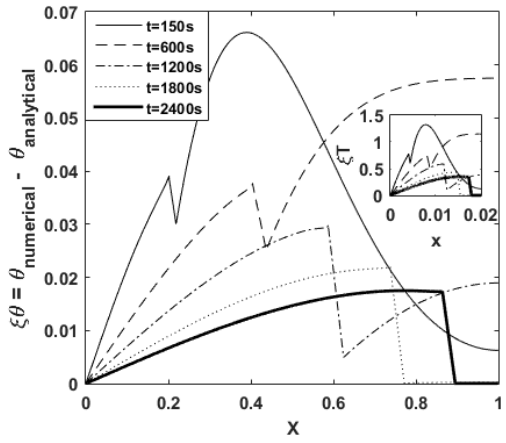

Figure 2.3 : Absolute error analysis of ND and dimensional(inset) temperature with space at different time instants.

equation (Eq. 2.2, 2.8), the finite volume based numerical model couples between the temperature (T) and liquid fraction (f_l) at specific grid points by means of enthalpy updating method. The enthalpy updating method is essentially a numerical scheme that involves omission of neighboring temperature effects on enthalpy updating at a particular grid point while using a relaxation factor to compensate for this omission. Since θ_ϕ in the solid and liquid domain (figure 2.2(b)) are linear and exponential respectively, even a slight mismatch between the interface location leads to a comparatively large deviation in temperature profile. However, the difference in results obtained from these two models are found to be within permissible limit ($\sim 100\ \mu m$ for X_i^*, and 6.5% for θ_ϕ) and the comparison can be considered to be satisfactory.

The confidence built by reasonable agreement of predictions by these two models motivated us to apply the proposed semi-analytical model for case studies involving volumetric expansion and shrinkage ($\rho_s \neq \rho_l$). The proposed semi-analytical model is verified by two case-studies relevant to volumetric expansion and shrinkage respectively. For volumetric expansion, solidification of water has been chosen as the model problem, while for shrinkage, solidification of paraffin (P116) is considered.

Variation of θ_ϕ, X_i^*, and L^* with ND time F_o during solidification of water is shown in figure 2.4(a). The initial temperature T_i, cold side temperature T_c, initial domain length L_0 and

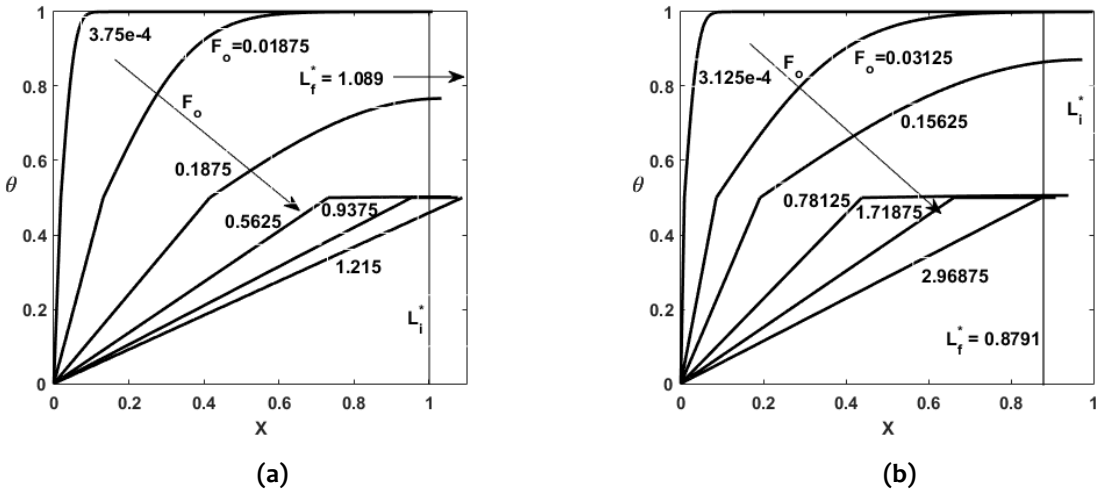

Figure 2.4 : Spatial variation θ_ϕ at different time instants for solidification of: (a) water considering volumetric expansion, and (b) paraffin considering shrinkage.

all the thermo-physical properties apart from ρ_s and ρ_l are chosen to be same as the validation problem. $\rho_s = 918\ kg/m^3$, and $\rho_l = 1000\ kg/m^3$ for water have been considered for the present case study. The temperature gradient at the interface decreases abruptly in the liquid domain (figure 2.4(a)), which is physically consistent with Stefan equation (Eq. 2.2, 2.8). Also, X_i^* can be identified by this sudden decrement of gradient in θ. From figure 2.4(a), it is also to be noted that although the initial value of L_0^* is unity, L^* keeps increasing from its initial value as the solidification process progresses in time denoting the volumetric expansion. After complete solidification is obtained, the final value of L^* is found out to be $L_f^* = 1.089$, which is consistent with the mass balance $\rho_l L_0 = \rho_s L_f$ where, L_0 and L_f are initial and final dimensional length of the domain.

Case study 2 involves solidification of paraffin (p116) for which $\rho_s > \rho_l$ and the solidification process is characterized by shrinkage. Thermo-physical properties of solid and liquid paraffin (melting temperature $T_m = 329.16\ K$ at atmospheric condition) are as follows: $k_s = 0.29\ W/mK$, $\rho_s = 910\ kg/m^3$, $c_{ps} = 2400\ J/kgK$, $k_l = 0.2\ W/mK$, $\rho_l = 800\ kg/m^3$, $c_{pl} = 2000\ J/kgK$, and $h_{sl} = 195\ kJ/kg$, while (T_i) and (T_c) are chosen to be $T_i = 339.16\ K$, $T_c = 319.16\ K$ and the L_0 is considered to be $L_0 = 20\ mm$. Variation of θ_ϕ, X_i^*, and L^* with ND time F_o during solidification of paraffin is shown in figure 2.4(b). Similar to the case study with water X_i^* in figure 2.4(b) can be identified by the location where gradient in θ changes abruptly. In figure 2.4(b), gradual decrement of L^* with increasing F_o confirms that the shrinkage phenomena is successfully captured by the model. Once again $L_f^* = 0.8791$ confirms the overall mass balance.

Finally, the models with and without considering volume expansion/shrinkage effects are compared in terms of evolution of solid-liquid interface with time for water and paraffin in figure 2.5. It is pertinent to mention here that solidification time for water is much lesser than that of paraffin as $k_{sw} >> k_{sp}$ and $k_{lw} > k_{lp}$, where k_{sw}, k_{lw}, k_{sp}, and k_{lp} are solid and liquid phase thermal conductivity of water and paraffin respectively. From figure 2.5 it is evident that the time required to obtain complete solidification of water is under-predicted if volumetric expansion is not considered, on the other hand no-shrinkage consideration significantly over-predicts the total solidification time for paraffin. The increment of required time duration for complete solidification of water and decrement of the same for solidification of paraffin predicted by the propose volumetric expansion/shrinkage model are physically consistent as volume expansion effectively increases the total length of the domain to be solidified, while shrinkage effectively reduce the total domain length.

It is evident from the above study; the semi-analytical model is capable enough to solve

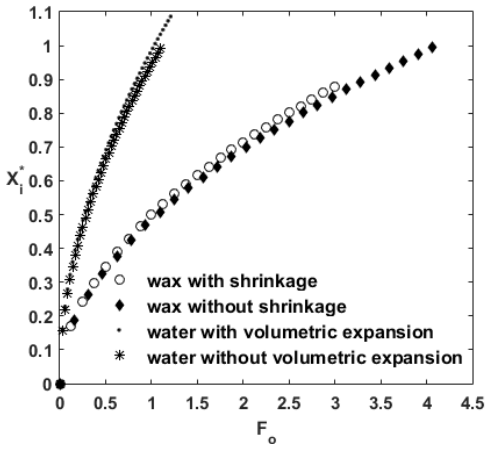

Figure 2.5 : Solid–liquid interface growth with time for water and paraffin

the problems where cooling conditions are known, and corresponding crystal growth rate and temperature distribution within the domain are to be estimated. However, the controlled crystal growth during experimentation can only be obtained if prior knowledge of the cooling condition is obtainable. Thus, the next chapter concerns problems where boundary condition corresponding to time-dependent crystal growth is approximated.

2.4 SUMMARY

A semi-analytical 1-D transient heat diffusion model is developed to predict the effect of density difference between solid and liquid phases during solidification of pure substance. The semi-analytical model is first validated for finite domain without considering volume expansion/shrinkage effect by comparing the results with those obtained from existing enthalpy updating based numerical model. Once reasonable agreement from the validation is obtained, case studies pertaining to volumetric expansion and shrinkage are performed. Case study corresponding to volumetric expansion is performed by applying the proposed model to predict temperature, interface and overall domain length during solidification of water, while solidification of paraffin is chosen for case study associated with shrinkage. The predicted time duration for complete solidification by proposed model considering volumetric expansion ($\rho_s < \rho_l$) is found out to be more than that without considering volumetric expansion ($\rho_s = \rho_l$), while reverse is found to be true for case study involving shrinkage ($\rho_s > \rho_l$), and both the results successfully captures physically consistency.

…